Improvement in the spatial resolution for imaging with fast neutrons

E. H. Lehmann, D. Mannes, M. Strobl, Paul Scherrer Institut, Lab. Neutron Scattering & Imaging

B. Walfort, RC Tritec, Teuffen, Switzerland

A. Losko, B. Schillinger, M. Schulz, TU München, MLZ, Garching, Germany

S. Vogel, D.C. Schaper, C. Gautier, D. Newmark, Los Alamos National Laboratory, USA

ABSTRACT

We report on the realization of an improved concept for the detection of fast neutrons using a specific setup of scintillators with the aim to overcome limitations in spatial resolution. While fast neutron imaging (FNI) is a technique to investigate very thick material layers in transmission mode, currently there is a limit in the spatial resolution at ~ 1 mm, which hinders the performance for the detection of features like cracks, material damage or pores in large objects (>> 1 cm^3). The improved concept presented here is based on the separation of the converter material from the scintillation layer in a suitable way,which was successfully tested and referenced to the standard devices at the NECTAR facility (FRM-2, MLZ, Garching) under realistic beamline conditions. The results imply a break-through in enabling detection of structures on the order of 0.2 to 0.5 mm (a more precise estimation is not possible due to other resolution determing factors in a realistic setup). Potential additional improvements are discussed.

Keywords: fast neutrons, scintillation detector, spatial resolution, transmission, neutron scattering, recoil protons, camera based setup

1. Introduction

Neutron imaging has been established at many neutron sources around the world providing sufficient performance and beam intensities [1]. Today, high source, instrument and detector performance as well as the implementation of modern imaging techniques [2] qualified neutron imaging as a valuable research tool but also for numerous industrial applications with regards to non-invasive investigations of components, materials and processes.

Most of the studies in neutron imaging are performed with thermal (around 25 meV in energy, 0.18 nm in wavelength) and cold neutrons (around 3 meV in energy, 0.3 nm in wavelength). There are several reasons for this fact: (a) the highest contrasts between materials under investigation can be found in these energy/wavelength ranges; (b) these energies match the excitation energies in condensed matter and the corresponding wavelengths match the atomar distances in solid state materials making thermal and cold neutrons outstanding probes for condensed matter science (c) the detection probability is highest within these low energy ranges.

However, all available neutrons generated either by nuclear fission or within nuclear reactions driven by accelerated particles have initially a high energy of some MeV and above, depending on the particular nuclear reaction. To obtain thermal or cold neutrons, a moderation process utilizing collisions for suitable light nuclei (H, D, C, …) is required which can slow down the high energy neutrons by many orders of magnitude. This is a common procedure in most neutron research labs where multiple beams are extracted from the source simultaneously.

Moreover, the initially produced fast neutrons have characteristics advantageous for some imaging applications, but have been utilized only in a few cases in a dedicated manner. One dedicated

This document is the accepted manuscript version of the following article:
Lehmann, E. H., Mannes, D., Strobl, M., Walfort, B., Losko, A., Schillinger, B., … Newmark, D. (2021). Improvement in the spatial resolution for imaging with fast neutrons. Nuclear Instruments and Methods in Physics Research, Section A: Accelerators, Spectrometers, Detectors and Associated Equipment, 988, 164809 (10 pp.). https://doi.org/10.1016/j.nima.2020.164809

instrument for imaging with fast neutrons is NECTAR [3] at the FRM-2 research reactor, which will be described in more detail below. It provides maybe the highest performance of corresponding instruments with respect to beam intensity, collimation and infrastructure. Other instruments include such at sources based on (D-D) or (D-T) fusion reactions [4] or accelerator driven sources, some of which are still under consideration and construction [5].

Beside problems with the beam properties (background by gamma radiation, thermalized neutrons and beam collimation) there is a higher shielding demand, the influence from scattered neutrons and the limited efficiency of the neutron imaging detectors which together render the technique highly non-trivial to establish. However, there is also the advantage of the fast neutrons to penetrate any material much better than low energy neutrons or X-rays. This in turn allows to investigate and analyse much thicker layers of structures and dense matter with fast neutrons.

The interactions with fast neutrons differ much from those with low energy neutrons. There is no strongly absorbing material for high neutron energies. All neutron interactions are dominated by several kinds of scattering and by the generation of secondary particles and corresponding (gamma) radiation. In addition, the interaction probability is generally low, indicated by cross-sections of only a few barn for all kinds of reactions and materials. This is the reason for the high penetration power on the one hand, but the limited detector efficiency on the other hand.

For the development of fast neutron imaging (FNI) towards a high-performance tool for academic and industrial applications, it is necessary to optimize the detection efficiency highest while simultaneously improving and maximizing the spatial resolution capability. Here we report results of initial tests of a new scintillator concept focused on the improvement of spatial resolution in imaging with fast neutrons. Measurements were performed at the dedicated imaging instrument NECTAR utilizing its radiography and tomography modes of operation. Successful tests led to immediate commercialization of the novel scintillator screens which improve the applicability of fast neutrons for imaging in research and for industrial usage.

2. Principles of Imaging with fast neutrons

The interaction probability of neutrons with matter is described by the available cross-section data. The collection of these data is performed since many years on a high level. Apart from a general physics interest, the development of nuclear power reactors, in particular also e.g. fast breeder reactors, was a driving force for extensive research and the establishment of corresponding data bases like ENDF/B or JEF [6, 7].

Fig. 1 representatively shows the cross-section data of Al over an extended energy range from 10 MeV down to the thermal neutron range of meV. Comparing the relevant data with respect to thermal neutron imaging with that for fast neutron imaging the following differences become aparent:

- The total cross-sections in the thermal range (< 0.4 eV, as definded by the Cd-cutoff) are generally much larger than at 1 MeV
- There are two competing reactions: neutron absorption and neutron scattering, which are of the same order of magnitude for thermal neutrons. Only for some materials (Cd, B-10, Gd, …), absorption is significantly higher than scattering.
- In the MeV region there is nearly no absorption and scattering of neutrons clearly dominates. The higher the neutron energy, the more exotic reactions (n-p, n-α, n-xn, …) are initiated, however with only low probability.

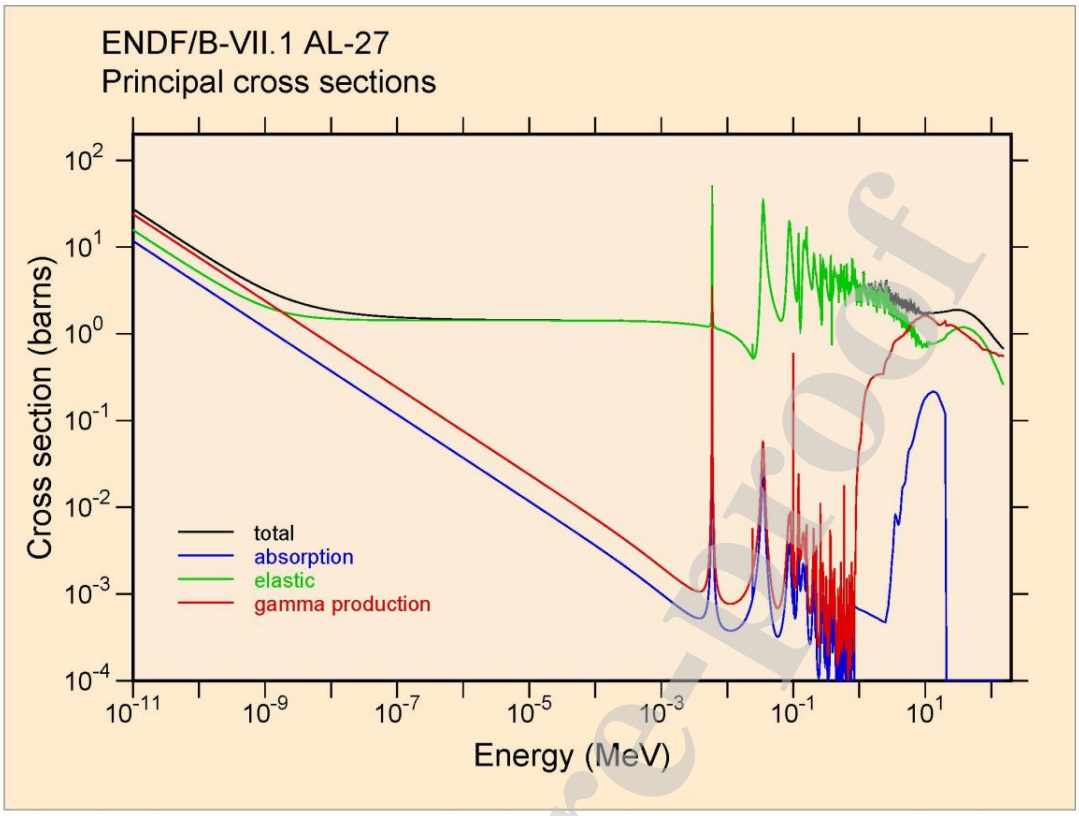

Fig. 1: Cross-section data for the interaction of neutrons with Al over the energy range from meV to MeV for the different reaction modes (data: ENDF/B-VII); the logarithmic scale has to be noticed for understanding!

This has consequences for the detection process, but also for the interpretation of data from FNI. Because neutrons do not carry an electric charge, their detection has to be achieved via a secondary reaction which enables an ionization processes. This way, a charge or light emission event can be detected. In the case of thermal neutrons, a primary neutron absorption process in Li-6, B-10, He-3 or Gd is used for the conversion. This does, however, not work efficiently for fast neutrons due to the lack of strong neutron absorbers in this energy range.

Thus, the scattering reaction with hydrogen, creating recoil protons, is one of the most efficient conversion processes for the detection of fast neutrons. The recoil proton (the hydrogen nucleus itself) is charged and entails secondary reactions. In the past, special photographic films were used for the subsequent detection in imaging with fast neutrons, which is a very slow procedure for obtaining the final image. Today digital imaging detectors [8] have repaced the film method completely. Here, the key component for neutron detection is a light emitting scintillator screen.

Due to its very high light emission efficiency, the scintillation material most commonly used is ZnS. It can additionally be doped with Ag or Cu for shifting the emission spectrum to fit to a maximum spectral photon sensitivity of the utilized sensor, in general a semi-conductor CCD, CMOS or a-Si device. Although this method has been used for many years, no systematic investigation has been reported for a long time in order to optimize this component, neither with respect to efficiency nor for improved spatial resolution. In many cases, screens were custom made by the respective facilities and only individual pieces have been produced.

Only recently a study has been published focusing on the properties of such scintillator screens for fast neutrons [9]. It was based on products from the company RC Tritec [10] and investigated the specific characteristics of efficiency, spatial resolution and gamma sensitivity in a systematic manner. The results show that the thickness of the homogenous mixture of the hydrogen-rich material (polypropylene) with a certain amount of ZnS goes influences the light emission linearly over a range of a few milli-meters. However, the thickness of the homogenous plates impairs the spatial resolution correspondingly. Therefore, a compromise between efficiency, i.e. exposure time and statistics, and spatial resolution has to be made carefully for every specific application. In the respective study, the edge-spread functions of the used scintillators implied achievable resolutions between 1.5 and 2 mm.

To improve the situation and enable better spatial resolution a different detection concept is required because the imaging sensor, the beam geometry and the scattering at the samples are less limiting factors.

3. Scintillator Screen Concept

As mentioned above, the approach of homogenous mixtures of proton-recoil converters with the light emitting material limits the resolution to the range of the thicknesses of the scintillator plates, i.e. to a few millimeters.

The improved concept of a higher resolving screen separates the hydrogenous converter material from the scintillation layer, by applying the scintillator onto a PE plate. The plastic part is firstly penetrated by the neutrons creating recoil protons. Only recoil protons, which are able to reach the scintillation material can contribute to the final image. In this way, multiple neutron scattering in the hydrogenous layer is suppressed and the inherent blurring is considerably reduced.

It has to be acknowledged, that similar approaches have been proposed earlier [11, 14], but no realization and application have been reported yet.

The study presented here had two stages. Initial principal tests varied not only the thickness of the PE plate but also the type of scintillating material, and were performed at a pulsed beamline of the Neutron Scattering Center of the Los Alamos National Laboratories (LANL). Based on these tests a detailed performance assessment of a screen manufactured with the experience of the initial study has been undertaken at the NECTAR instrument of the Technical University Munich (TUM).

4. Initial study at LANL

First tests were carried out at the pulsed spallation neutron source at Los Alamos National Laboratories at the Lujan Center for Neutron Scattering (LANSCE). Images were taken at Flight Path 60 Right (FP60R) usig a light-tight detector box [13]. After the neutrons passed through a step wedge designed for resolution studies with fast neutrons they were incident on the scintillator screens being tested. The resulting light was reflected off of a mylar pellicle mirror into a Nikon lens and collected by a PiMax4 camera. A Thorlabs USAF resolution target was used to focus the PiMax4 camera on the front surface of the scintillator, and reproducible exchange of the tested scintillators was enabled using a three-point kinematic mount. The camera was timed such that the images were taken using 3MeV-14MeV neutrons (integrated over all energies) due to the well-defined time-of-flight from the neutron source to the detector at about 21 meters downstream. The pulse frequency was 120 Hz and the utilized detection duration in each pulse was only 632 ns. Three sets of images were recorded for each scintillator tested: flat fields = open beam (OB), dark current (DC), and the images of the copper step wedge object in the beam. For each set of images, 200 individual frames (images) were recorded within about 7 minutes. Each set of 200 images was then collated into a single image. The dark current image was subtracted from the images of the resolution test object and the flat field, and the latter was

subsequently used to normalize the former. A typical image, corrected for DC and normalized by the OB is shown in Fig. 2 together with the Cu test device for determining the edge blurring, thus the spatial resolution.

A standard ZnS doped polypropylene plate (2.4 mm thick) was used as reference to compare with the results for the novel polyethylene (PE) plates with different thickness (2 to 10 mm) combined with a thin layer of scintillator or conversion/scintillation material of 0.15 mm thickness. For the latter layer a choice of ZnS:Cu, LiF-ZnS:Cu, or GADOX in the form of Gd2O2S:Tb and Gd2O3Tb were used.

The results imply a loss of efficiency of around a factor of three but a gain in resolution of up to a factor of 2 for some of the novel screens. The resolution was assessed in the form of the full-width-half-maximum (FWHM) of the measured edge spread. A summary of data evaluation results with regards to the spatial resolution capability of the screens are given in Table 1. The resolution degrades overall with increasing thickness of the PE substrate. The ZnS:Cu screens including LiF appear to display superior resolution. Note, however, that due to limited and not fully defined beam collimation at this instrument and a relatively large sample to detector distance of around 20 cm, these results for the resolution are relative with respect to the standard screen, and measured improvements by the new screens might be limited by the geometric blur of the image.

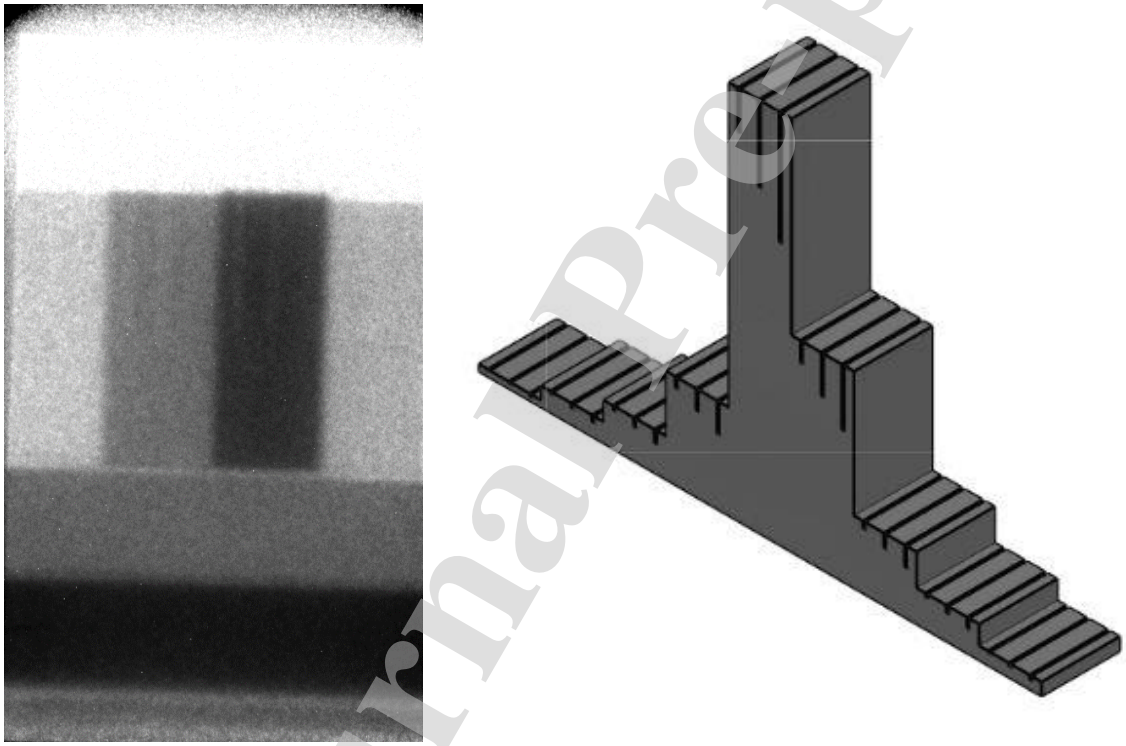

Fig. 2: Open beam corrected transmission image (left) of the Cu test object, lying perpendicular to the beam direction with the highest step of 60 mm; these data were used for determination of the "full widths half maximum" (FWHM) data in the table below

Table 1: Evaluation of the data from the scintillator tests at LANL using fast neutrons

sample	central averaged intensity	FWHM [mm]
PE2mm_ZnSCuLiF	**1274**	1.12
PE3mm_ZnSCuLiF	**1306**	1.18
PP3mm_ZnSCu	**1495**	1.43
PE5mm_ZnSCuLiF	**1456**	1.22
PE2mm_Gd2O3Tb	**975**	1.17
PE3mm_Gd2O3Tb	**1038**	1.48
PE5mm_Gd2O2STb	**1115**	1.90
PE10mm_Gd2O2STb	**1220**	1.73
PP ZnS Cu reference	**3479**	2.20

These trends encouraged to perform further tests with correspondingly improved screens at the well defined beam of the NECTAR instrument at TUM.

5. NECTAR instrument for fast neutron imaging

One of the neutron imaging instruments at the FRM-2 research reactor of TU München in Garching is NECTAR, sharing the beamline with a medical treatment option and a facility for prompt-gamma activation analysis using fast neutrons (FANGAS) [12].

The fast neutrons are produced by fission in a U-235 converter plate, which is installed in front of the beam port SR10. The thermalized neutrons from the moderator tank around the only fuel element create fission neutrons with the typical fission spectrum peaking at about 1.8 MeV and a tail towards lower neutron energies. Because also gamma radiation is produced in the fission process the extracted beam at SR10 is strongly contaminated by gamma radiation.

Nevertheless, NECTAR is one of the very few instruments able and optimized to perform investigations with fast neutrons, in particular radiography and tomography. The high initial beam intensity allows to trade flux for resolution and thus high beam collimations can be achieved with collimation ratios tunable from about 200 to 800. In a recent upgrade, NECTAR was equipped with a state-of-the-art digital detection system, a comfortable sample manipulator, an adequate shielding and filter and shutter options to tune the beam. In addition, the U-235 converter plate can be removed for optional thermal neutron imaging.

At the most commonly used collimation ratio of 200 the fast neutron flux corresponds to ~10^7 cm^{-2} s^{-1}. Images of good quality and with resolutions of about 1 mm can be obtained with the conventional setup (see below) within seconds to minutes depeding on the requirements and samples. A tomography run lasts typically for some hours.

Due to high flexibility, performance and obtainable data quality digital imaging detectors based on a highly sensitive camera viewing the neutron sensitive scintillator screen via a light reflecting mirror (s. Fig. 3 left) have become a general standard at all modern neutron imaging instruments. A double-mirror setup (right part of Fig. 3) is used at NECTAR because the background by scattered neutrons and migrating gamma radiation need to be suppressed at the camera position in order to avoid permanent chip damage and to reduce the level of “white spots” in the images, i.e. to improve the data quality. The light path from thr scintillator to the camera is in a light-tight box, which is sealed at the scintillator position simply with Al tape. This way, scintillator screens can be exchanged easily (Fig. 3 right).

The used camera was a cooled CCD (-100°C) ANDOR-Icon L with 2048 x 2048 pixels of 13.5 x 13.5 μm^2. A photographic lens (Zeiss) of f=135 mm and NA=2 covered a field of view (FOV) of about 20 cm * 20 cm, which corresponds to an effective pixel size of the detector system on the order of 0.1 x 0.1 mm^2, much smaller than the inherent resolution of >1mm of the standard scintillator screen (PP plate filled with 30% of ZnS).

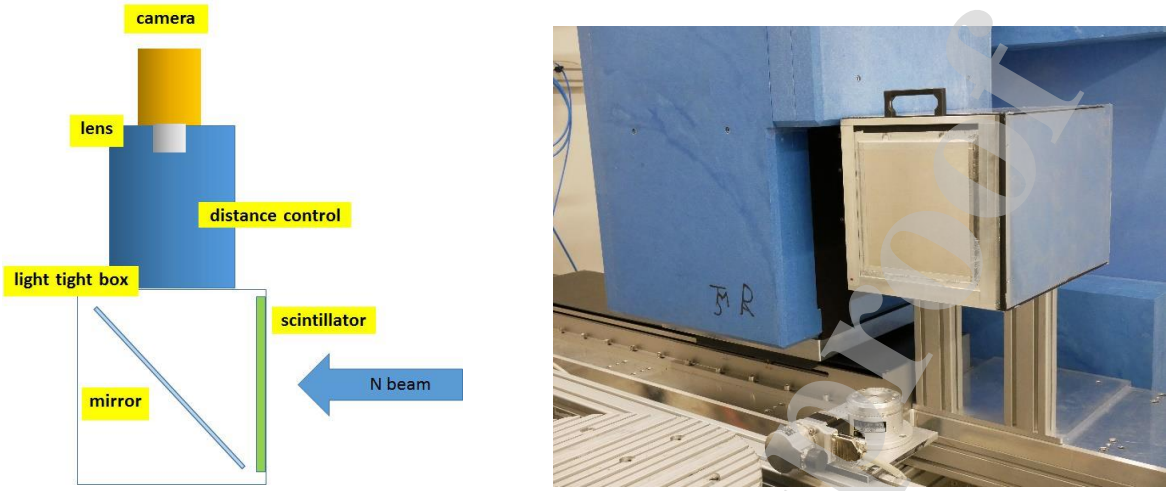

Fig. 3: Principle setup of the used camera detector (left); light tight box with scintillator and two mirrors (one in the box on the right, the other inside the blue shielding block on the left) at the NECTAR beam line of FRM-2, TU München (right); the camera is placed behind the blue shielding block, the beam comes from the left side

6. Test measurements at NECTAR: Final assessment

It was possible to use NECTAR in February 2020 for test measurements with an optimized screen with 3 mm poly-ethylene combined with a 0.06 mm Ag doped ZnS layer. This means a medium thin PE plate was used with regards to the initial test at LANL. However, the scintillator was chosen significantly thinner than in the initial study, expecting a corresponding further improvement in resolution, traded against some efficiency. The same standard screen as before was used as reference. The inherently given effective pixel size of the detector system of about 0.1 mm was sufficiently small to evaluate improvements in the spatial resolution of the scintillator screens.

Several test objects were used to study the scintillator performance and to evaluate the spatial resolution features:

- Laser melted plastic device with an embedded Siemens-star structure and horizontal and vertical slits with 0.8 mm distance (1.6 mm period) (Fig. 4)
- Steel object with holes of diameters between 1 mm and 6 mm and slits, either 1 mm (2 mm period) or 0.5 mm (1 mm period) (Fig. 5)
- Al, steel and Cu cubes with inner pyramidal structures (Fig. 6)

Fig. 4: Plastic sample with embedded structures (size: 50 mm, 50 mm, 80 mm); 1.6 mm period in the slit regions

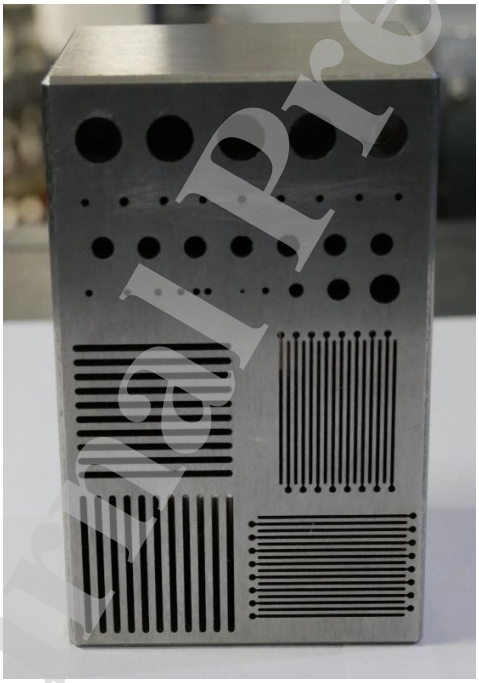

Fig. 5: Steel object with line and hole structures (size: 50 mm; 50 mm; 80 mm); 1.0 mm period in the smaller slit regions

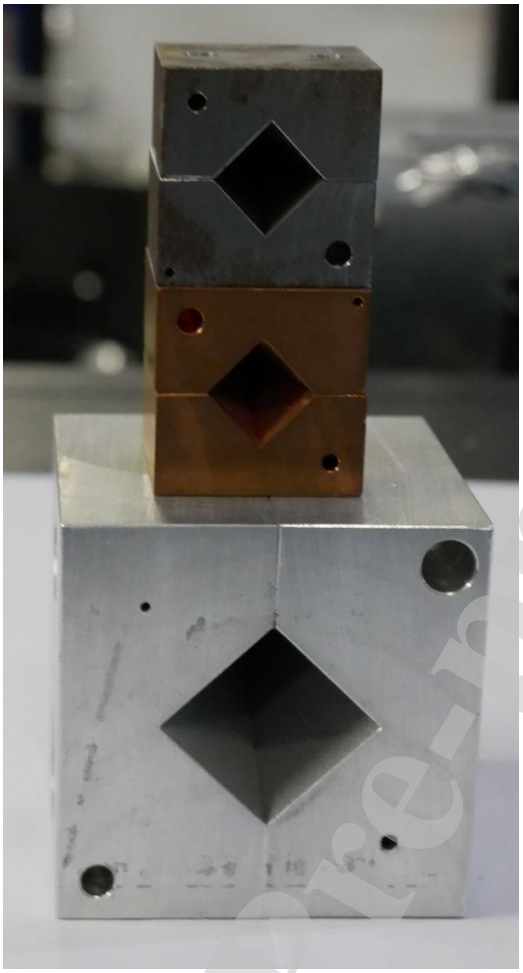

Fig. 6: Metal cubes of steel (25 mm), Cu (25 mm) and Al (50 mm); the samples consists of semi-cubes and contain an inner pyramidal empty space, kept together with screws

The measurements were performed by recording five frames (images) of 30 s exposure for each experimental set-up as well as for open beam (OB, without sample) and dark current (DC, shutter closed) measurements. The resulting image data were spot cleaned and averaged over the five frames before the equally treated DC image was subtracted from the images. The OB images were subjected to the same data treatment procedure, before they were used for image normalization.

6.1. Radiography Results

Apart from a initial visual comparison of the obtained image data detailed data analyses was performed to obtained the spatial resolution capability of the novel screen. A severe issue for the evaluation of the spatial resolution through a assessment of edge-spread functions of images produced with fast neutrons is the lack of strong absorber materials, which would allow to produce a clear, flat absorption edge. Instead, it is necessary to use thick material layers to achieve sufficient attenuation and thus high contrast in a distinct edge function recorded in an image. The alignment of an edge with significant extension along the beam together with the divergence of the beam and scattering effects imply an intrinsic blur due to the imaging geometry, which hinders a straight forward assessment of the intrinsic detector resolution alone.

All three test samples were transmitted by significant fractions of the fast neutron beam. The obtained image data are of reasonable quality and within the dynamic range of the detection system. The

optimum alignment of the structures in beam direction in order to minimize geometrical blur was nevertheless challenging.

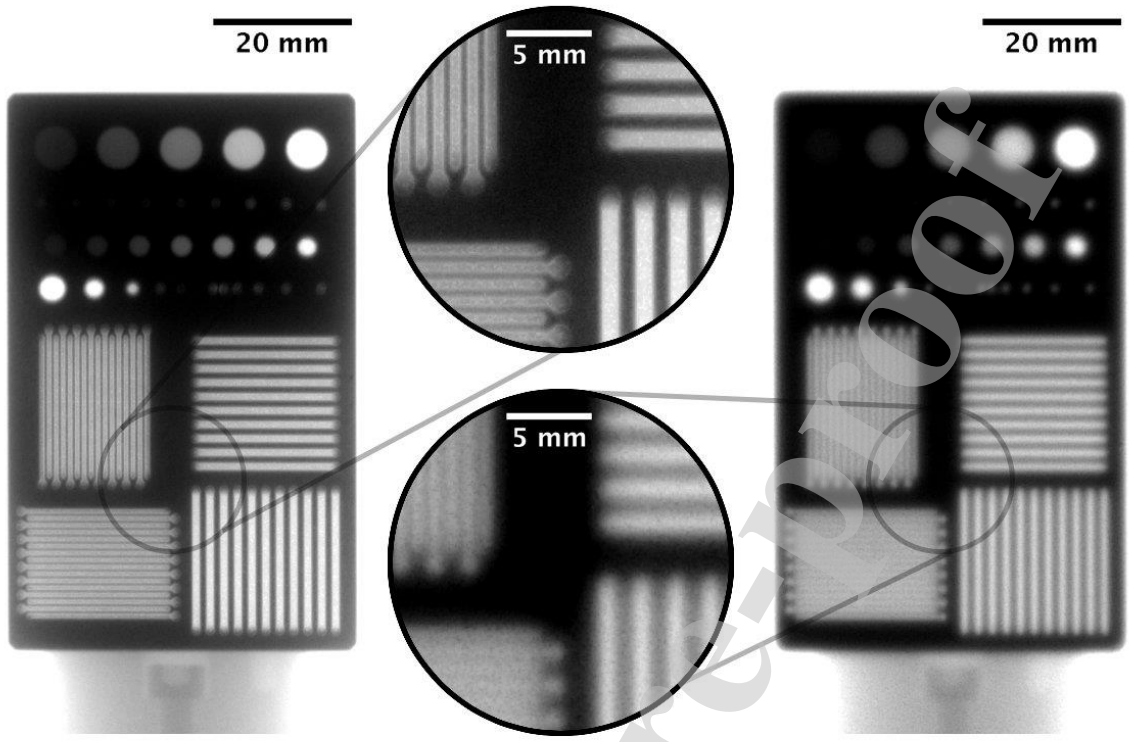

Fig. 7: Comparison of the transmission images obtained with the standard scintillator (right) and the new device, described in this paper (left). Enlarged images of the lammerlar structure of the test object are shown in the center.

All three test samples demonstrate impressively the progress achieved with the new screens as can be observed easily in the Figs. 7 to 9. A more quantitative comparison is presented through line profile data plotted in Fig. 10 and 11 and extracted from the regions indicated in Fig.7 and 8, respectively.

Next to a visual comparison of the obtained image data, the spatial resolution was obtained using the modulation transfer function (MTF) at 10% [Boreman, Glenn D. *Modulation transfer function in optical and electro-optical systems*. Vol. 10. No. 3.419857. Bellingham, WA: SPIE press, 2001].

Using the MTF at 10% applied to the lammelar features as illustrated in Fig. 7, the resolution for the old system was determined to be 374um and 170um for the new sytem, respectively. This yields an increase in spatial resolution for the new system by a factor of 2.2. The obtained MTF curve is shown in Fig. 8.

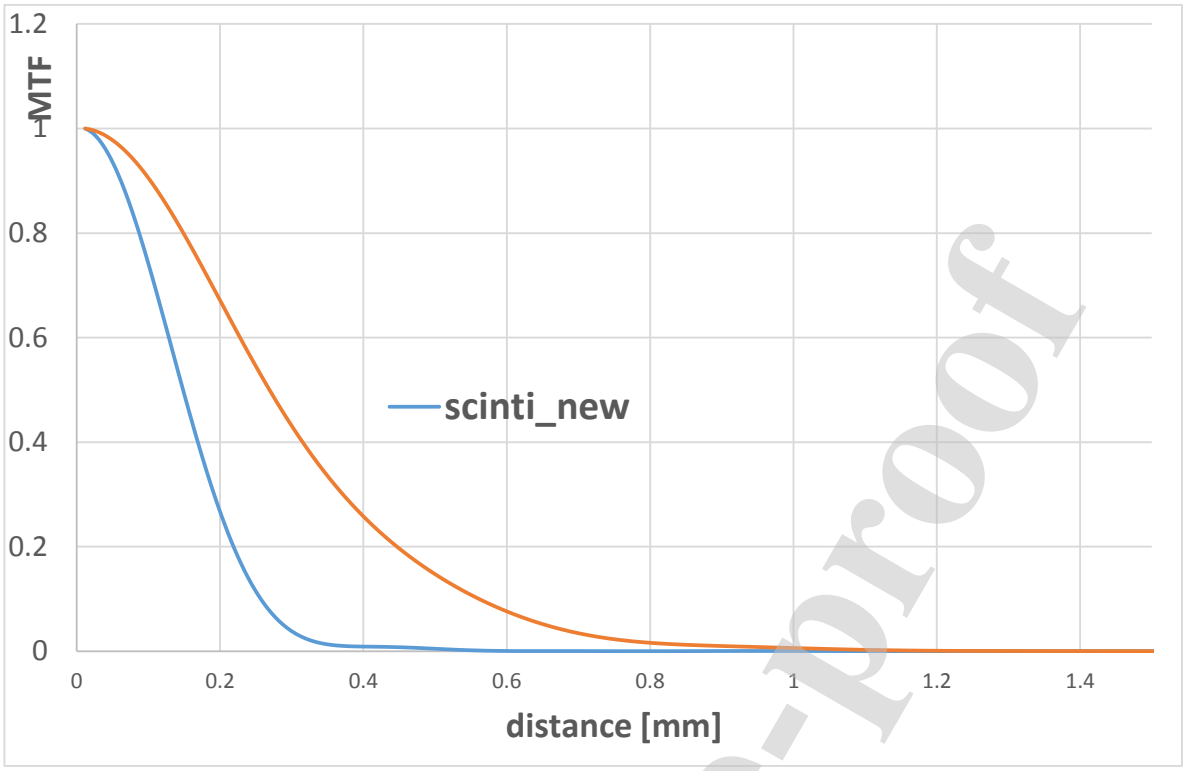

Fig. 8: MTF data from the evaluation of the slit region for the old and new scintillator screens

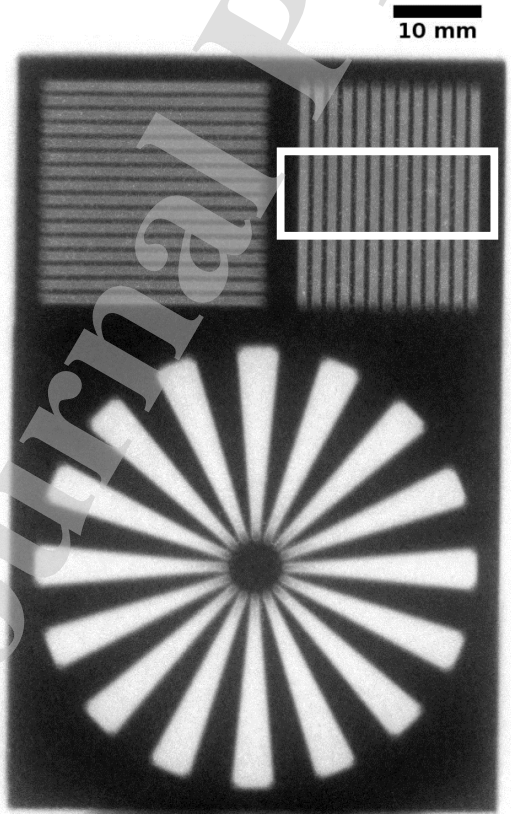

Fig. 9: **T**ransmission image data of the PE test object from Fig. 4; obtained with the new device; the region of the profile in Fig. 11 is indicated

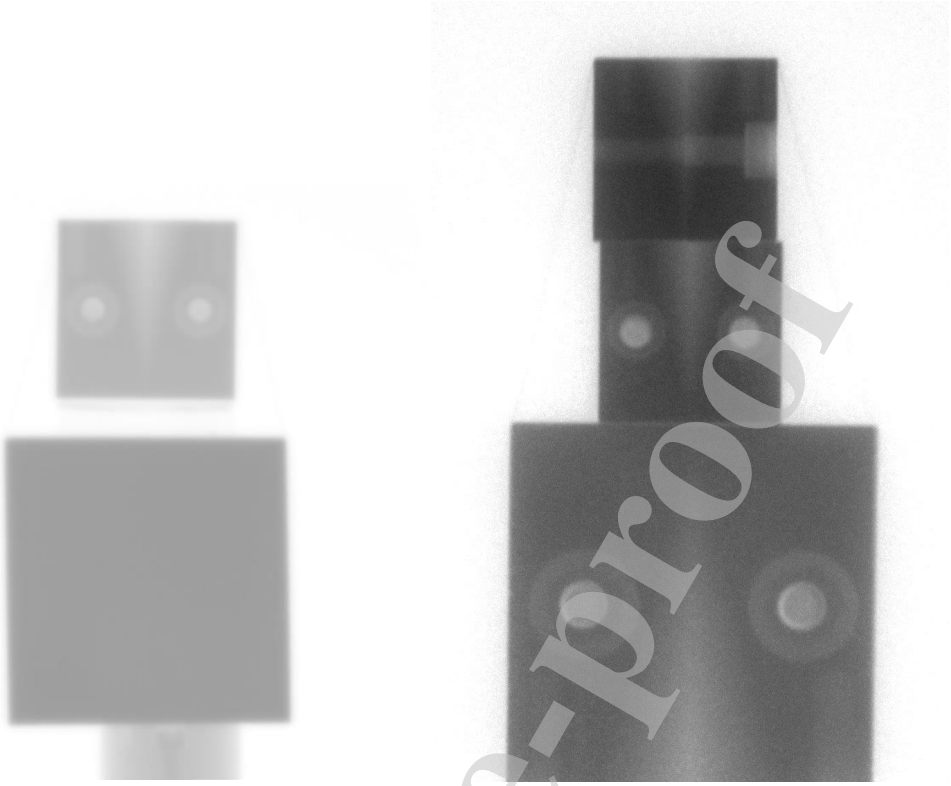

Fig. 10: Comparison of the transmission image data of the cube test object from Fig. 6; left: standard scintillator, right: new device

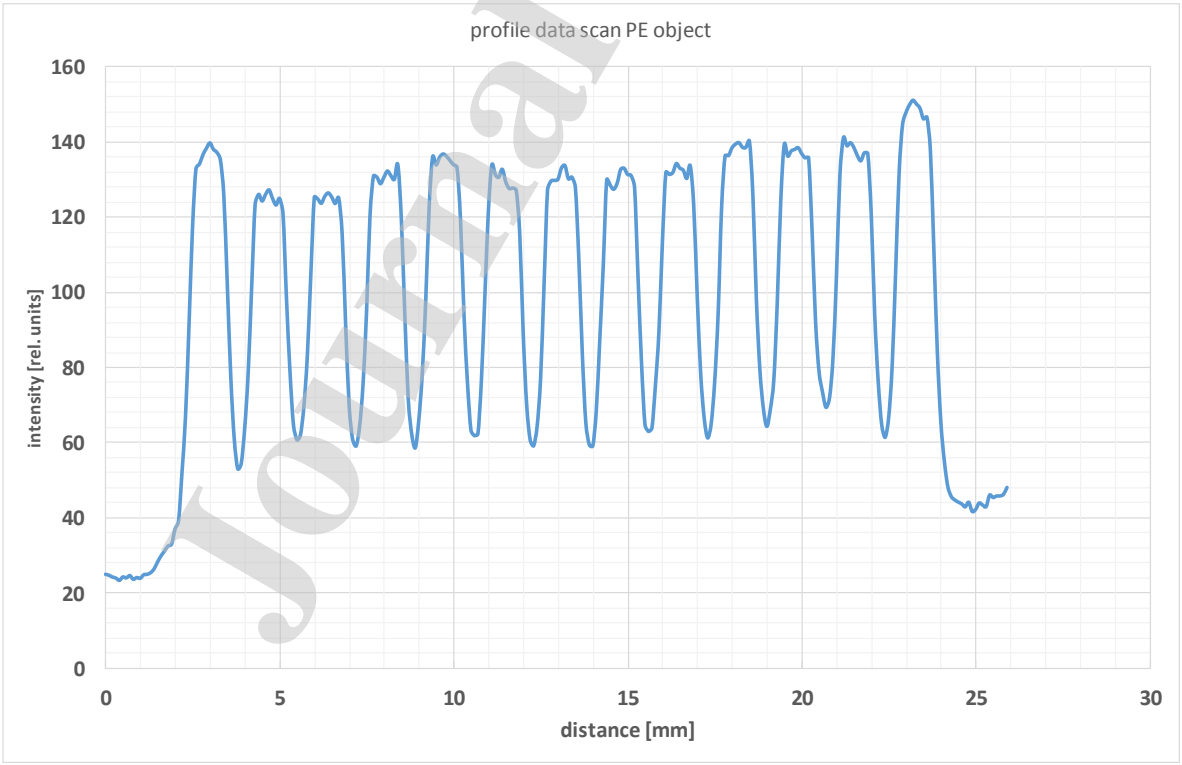

Fig. 11: Profile of the region from Fig. 9 of the PE test object

6.2. Tomography Results

By means of tomography measurements access to the three-dimensionally spatial resolved attenuation properties of a sample is obtained. Here the method enables to asses the resolution capabilities for three-dimensional measurements and thus in the volume of samples. However, in tomography also the number of projection images recorded as well as the reconstruction algorithms applied influence the resolution. However, applying well proven sampling rules and strategies as well ad reconstruction procedures, the direct comparison between measurements with the standard screen and the novel screen is straight forward. Fig. 11 displayes a frontal 3D view of the tomographic volume of the plastic test object.

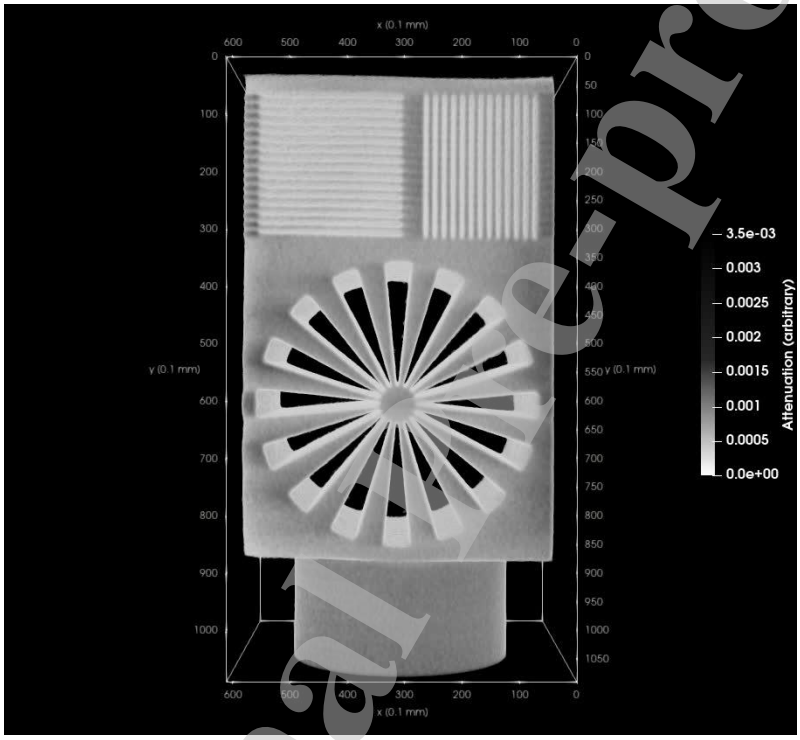

Fig. 12: Frontal view on the 3D data set of the plastic test object from Fig. 4

A comparison between the standard scintillator screen and the new screen in tomography is illustrated by corresponding cross sectional slices of the 50 mm Al cube sample (compare Fig. 6) with a pyramidal hole and connective srews in Fig. 12. On the left hand side the results with the new screen are juxtaposed to the corresponding results with the standard screenn and on the right hand side.

All three pairs of slices clearly demonstrate the superior resolution in particular at the edges and holes in the case of the new screen. The obvious higher noise level in the tomography data with the new screen is caused by the lower counting statistics in these measurements, due to the lower efficiency and light output of the novel screen.

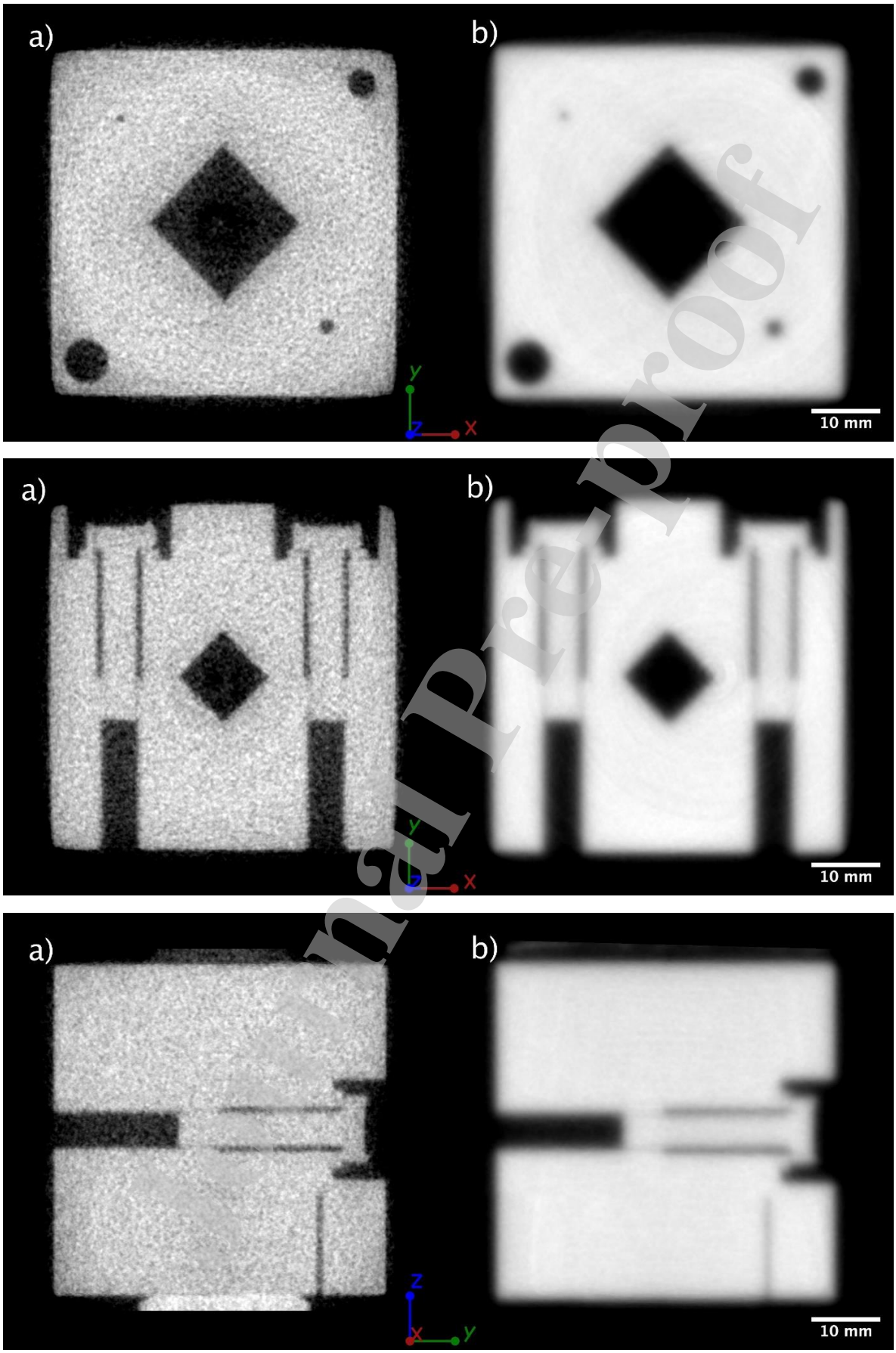

Fig. 13: Horizontal and vertical sclices through the 50 mm Al cube; left (a): using the new device, right (b): using the standard scintillator

7. Summary and outlook

A novel concept for high resolution scintillator screens has been introduced and tested. The concept of separated layers of a thick hydrogen rich layer creating recoil protons by scattering with fast neutrons and a thin scintillator layer could be demonstrated to have the potential to significantly increase spatial resolution in imaging with fast neutrons. A two phase study conveying an initial test with different layer thickness of PE and various scintillator material layers and a second phase assessing the performance of a subsequently improved screen has been performed. As a result a 2-5 -fold improvement in resolution as compared to a standard reference screen was achieved by a trade against a factor of about four in efficiency. The achieved resolution was quantified to 0.2 mm in radiography and 0.25 mm in 3D based on tomographic tests.

As a consequence of this work corresponding new scintillator screens for imaging with fast eutrons are already commercially available. However, further progress can certainly be sought by e.g. (i) optimization of the converter material by increasing the hydrogen density and (ii) utilization of structured scintillators for high detection efficiency but limited light spread.

Acknowledgements

We thank all involved persons for their assistance during and after the experiments who are not explicitely mentioned in the author's list, in particular Darcy Newmark from LANL, USA.

References:

[1] http://www.isnr.de/index.php/facilities/facilities-worlwide

[2] https://www.psi.ch/de/niag/neutron-imaging-techniques-and-methods

[3] T. Bücherl, S. Söllradl, NECTAR: Radiography and tomography station using fission neutrons, JLSRF 1, A19, DOI: http://dx.doi.org/10.17815/jlsrf-1-45

[4] https://phoenixwi.com/neutron-generators/high-flux-neutron-generator/dd-deuterium-deuterium-neutron-generators/#dd-neutrons

[5] T. Gutberlet et al., The Jülich high brilliance neutron source project – Improving access to neutrons, Physica B: Condensed Matter,Volume 570, 1 October 2019, Pages 345-348, https://doi.org/10.1016/j.physb.2018.01.019

[6] D.A. Brown et al., ENDF/B-VIII.0: The 8th Major Release of the Nuclear Reaction Data Library with CIELO-project Cross Sections, New Standards and Thermal Scattering Data, Nuclear Data Sheets, Volume 148, February 2018, Pages 1-142https://doi.org/10.1016/j.nds.2018.02.001

[7] https://www.oecd-nea.org/dbdata/jeff/

[8] E. H. Lehmann et al., Neutron imaging — Detector options in progress, 2011 JINST 6 C01050, doi:10.1088/1748-0221/6/01/C01050

[9] M. G. Makowska et al., Performance of the Commercial PP/ZnS:Cu and PP/ZnS:Ag Scintillation Screens for Fast Neutron Imaging J. Imaging 2017, 3, 60; doi:10.3390/jimaging3040060

[10] https://www.rctritec.com/de/szintillatoren/produkte.html

[11] R. Ambrosi et al., Large area microchannel plate detector with amorphous silicon pixel array readout for fast neutron radiography, Nuclear Instruments and Methods A, Volume 500, Issues 1–3, 11 March 2003, Pages 351-361, https://doi.org/10.1016/S0168-9002(03)00297-3

[12] M. Rossbach, FaNGaS: Fast NeutronGammaSpectroscopy instrument for prompt gamma signature of inelastic scattering reactions, Journal of large-scale research facilities, 1, A32 (2015) http://dx.doi.org/10.17815/jlsrf-1-54

[13] A. Swift et al., Time gating for energy selection and scatter rejection: high energy pulsed neutron imaging at LANSCE, Proc. SPIE 9595, Radiation Detectors: Systems and Applications XVI, 95950J (27 August 2015); doi:10.1117/12.2188440

[14] V. Dangendorf et al., Detectors for Energy-Resolved Fast Neutron Imaging, Elsevier Science https://arxiv.org/ftp/nucl-ex/papers/0403/0403051.pdf

Credit Author Statements

E. H. Lehmann acts as corresponding author in the name of all contributors and with the full right to make the needed changes.